

Influence of WS₂ content on high temperature wear performance of magnetron sputtered TiN-WS_x thin films

E.C. Serra^a, V.F.D. Soares^a, D.A.R. Fernandez^{a,*}, R. Hübler^b, K.R.C. Juste^c, C.L. Lima^d, E.K. Tentardini^a

^a Universidade Federal de Sergipe, Av. Marechal Rondon, S/N, São Cristóvão, SE, Brazil

^b Pontifícia Universidade Católica Do Rio Grande Do Sul – PUCRS, Av. Ipiranga, 6681, Porto Alegre, RS, Brazil

^c Instituto SENAI de Inovação Em Engenharia de Superfícies-ISIES/FIEMG, Avenida Cândido da Silveira, Horto, 31035-536, Belo Horizonte, MG, Brazil

^d Universidade Federal Do Piauí, Campus Min. Petrônio Portela, Ininga, 64049-550, Teresina, PI, Brazil

ARTICLE INFO

Keywords:

TiN-WS₂
High temperature wear
Self-lubricating coating
Thin films
Magnetron sputtering

ABSTRACT

TiN-WS_x thin films with varying WS_x content were co-deposited by reactive magnetron sputtering. GAXRD analyses showed that the addition of 4 at.% WS_x led to loss of crystallinity of TiN phase and a complete amorphous characteristic was manifested upon incorporation of 19 at.% WS_x. Nanohardness results indicated that TiN-WS_x containing 4 and 19 at.% WS_x presented 19.7 GPa and 18.4 GPa, respectively, following the rule of mixtures. Friction coefficient and wear rates measured in reciprocated tribological tests revealed that TiN-WS_x coatings present an improved tribological performance when compared to pure TiN thin film at room temperature, registering friction coefficient of 0.42 ± 0.05 and 0.19 ± 0.03 for samples with 4 and 19 at.% WS_x, respectively. Wear tests at high temperatures evidenced that sample with 4 at.% WS_x did not provide advanced protection to substrate at 343 K and above due to deterioration. On the other hand, coating with 19 at.% WS_x maintained low friction coefficient up to 343 K, registering an optimum wear rate of $0.86 \times 10^{-17} \text{ m}^2/\text{N}$ with no cracking occurrence.

1. Introduction

Dry machining tools such as drills, cutting inserts and gears can suffer significant modification in friction coefficient due to heat generated by surface sliding, greatly limiting the lifespan [1,2]. Aiming to prevent such issues, liquid lubricants have been extensively used. Nevertheless, usual inefficiency in vacuum situations and environmental aggressiveness have encouraged researches towards their reduction or elimination [3,4].

In this context, solid lubricants thin films have gained special attention in surface engineering. Graphite thin films, for instance, have shown friction coefficient values ≤ 0.2 against ceramic and steel counter-bodies [5,6]. Comparably, MoS₂ thin films - one of the solid lubricant protagonists - have been extensively applied in aerospace and dry machining applications, presenting coefficient values of about ~ 0.3 [7]. However, once the lubricity mechanism of solid lubricants is extremely dependent on ambient temperature, these lubricants lose efficiency over 673 K due to occurrence of oxidation.

On the other hand, tungsten disulfide (WS₂) has attracted attention

more recently [2,8–10] due to several advantages over traditional solid lubricants, such as higher molecular weight (providing better stability), lower oxidation rate at higher temperatures and maintenance of lubricant properties at severe conditions [9,10].

WS₂ lubricant effect derives mainly from its weak Van Der Waals bonds, which are easily rearranged between atomic layers when subjected to shearing forces. As a result, friction coefficient of such coatings in inert atmospheres can reach values as low as 0.1 against steel [11,12]. Notwithstanding, the low hardness of 3.6 GPa [13] combined with sensitivity to high temperatures and humid environments limits the applicability of WS₂ thin films in severe wear situations [9,14].

In parallel, titanium nitride (TiN) have been extensively applied as protective coating to different manufacturing tools mainly due to high hardness and chemical inertness, rendering significant optimization of wear and oxidation resistance [2,3,15,16]. Despite the excellent properties, TiN inherently possesses a high friction coefficient, varying between 0.7 and 0.9 against steel and carbides [2,16,17]. Since the intense friction of hard materials commonly lead to the production of residues, surfaces increment of friction coefficient and abrasive wear

* Corresponding author. Universidade Federal de Sergipe, Av. Marechal Rondon, S/N, Departamento de Ciência e Engenharia de Materiais, São Cristóvão, SE, Brazil.

E-mail address: daniel.angel0275@gmail.com (D.A.R. Fernandez).

<https://doi.org/10.1016/j.ceramint.2019.06.248>

Received 9 February 2019; Received in revised form 21 June 2019; Accepted 23 June 2019

Available online 25 June 2019

0272-8842/ © 2019 Elsevier Ltd and Techna Group S.r.l. All rights reserved.

are frequently observed, compromising TiN tribological performance [8,9].

An alternative to simultaneously reduce TiN friction coefficient and restrict WS₂ contact with humidity is the development of TiN-WS₂ autolubricant nanocomposite thin films. Recent literature show that combination of both materials improves WS₂ protection against oxidation, allowing more effectiveness to solid lubricant action while retaining significant hardness levels associated to TiN phase [9,12].

Nonetheless, special attention has to be given to WS₂ concentration in order to ideally equilibrate properties [11]. Some works report that TiN-WS_x thin films containing 4.9 to 61.5 at.% WS₂ present a reduction of TiN original friction coefficient from 0.60 to 0.25, maintaining optimum hardness levels [9,12]. However, tribological tests have only been carried out at room temperature so far, whereas industrial processes, such as dry machining, usually expose coatings to temperatures as high as 573 K [8].

In order to acquire a concrete knowledge concerning the applicability of TiN-WS₂ thin films in industrial scale, it is of extreme relevance to thoroughly analyze its tribological behavior at high temperatures, subject not yet described in the literature.

The present work reports on the investigation regarding the influence of 4 and 19 at.% WS₂ in tribological behavior of TiN-WS_x thin films at room temperature and at 343 K, 423 K and 573 K. Coatings were deposited by reactive magnetron sputtering and characterized by Rutherford Backscattering Spectrometry (RBS), Glancing Angle X-ray Diffraction (GAXRD), nanoindentation and tribology tests with ball-on-flat reciprocating tribometer. Wear zones were analyzed by optical profiler and Energy-dispersive X-ray Spectroscopy (EDS).

2. Material and methods

Pure TiN, WS_x and TiN-WS_x thin films were co-deposited by reactive magnetron sputtering in an AJA equipment, Orion 5-HV Sputtering Systems model, with direct current (DC) and radiofrequency (RF) power sources, where Ti (99.98%) and WS₂ (99.99%) targets were placed, respectively.

Polyethylene, silicon wafers and AISI 304 stainless steel (Ra = 6 nm) were used as substrates according to characterization techniques used. All substrates undergone ultrasonic baths in acetone for 30 min and were subsequently inserted in deposition chamber.

Distance from target to substrates was 120 mm and base pressure in deposition chamber was 1.3×10^{-5} Pa. Before depositions, targets were subjected to pre-sputtering with argon flow rate of 21 sccm, pressure at 4×10^{-1} Pa and 100 W applied in each target for 5 min in order to remove impurities or oxides from the surface. Working pressure was set at 4×10^{-1} Pa, Ar/N₂ ratio at 19/2 sccm, no bias voltage or external heating was applied to substrates. Ti target power was kept constant at 92 W, while WS₂ target was set at 90 W for pure WS₂ and 12 and 60 W for TiN-WS_x coatings. With these deposition parameters, it was possible to obtain the TiN/WS₂ concentrations desired for this work.

Samples deposited on polyethylene were deposited for 15 min resulting in thin films with approximately 100 nm thickness, which allowed better peaks separation in RBS analyses. Samples deposited on silicon wafer and AISI 304 stainless steel were deposited for 240 min to obtain thin films with thickness of 1 μm.

RBS analyses were performed in a 3 MV Tandemron equipment, using He⁺⁺ particles accelerated with 2 MeV and a silicon detector at 165° (resolution of 12 KeV). Thickness and elemental composition were estimated using RUMP software. GAXRD tests were executed using a Shimadzu XRD-6000 equipment with Cu-Kα radiation ($\lambda = 1.54 \text{ \AA}$) and grazing angle incidence of 1°.

Nanoindentation tests were carried out by Fisherscope HV 100 equipment with Berkovich indenter. In order to minimize the influence of substrate in the resulting values, a load of 10 mN was applied, reaching a maximum indentation depth of 40 nm. Hardness values were

calculated according to ISO 14577 standard.

Tribological characterizations were performed in a Bruker UMT Tribolab ball-on-flat reciprocating tribometer using alumina (Al₂O₃) spheres of 6 mm diameter. Applied test load was set up at 2 N and the sliding trail was 7 mm, with a slide frequency of 1 Hz. The tribological parameters used were determined based on earlier ball-on-flat reciprocating analysis realized on thin films [18,19]. Average friction coefficient values were registered after a running-in/stabilization period. Tests were executed during 1800 s varying temperature at 297 K, 343 K, 423 K and 573 K, with an initial relative humidity of 60%. Wear zones were analyzed by SEM and EDS with Jeol JCM 5700 equipment and wear volumes were obtained through a Bruker ContourGT optical profiler.

3. Results and discussion

3.1. Composition, structure and nanohardness analysis

As deposited TiN and TiN-WS_x thin films were characterized by RBS to determine coatings stoichiometry. A representative RBS spectrum treated with RUMP software obtained for the sample with 19 at.% WS_x is shown in Fig. 1. Similar spectra (not shown) were obtained for other samples. Carbon peak is related to polyethylene substrate, employed in order to avoid high background signals from Si and stainless steel used for other characterizations in the present work.

Titanium, nitrogen, tungsten and sulfur peaks related to the film can be identified, as well as oxygen. The latter is probably derived from residual O₂ and H₂O present in deposition chamber. Since oxygen concentration is lower than 6 at.% it tends to substitute nitrogen in TiN lattice, not causing modification of crystal structure nor the formation of oxides during deposition [20,21]. Table 1 presents the chemical composition and the approximate WS_x contents in TiN matrix for all samples. It is observed a sulfur deficiency in nanocomposite samples, phenomenon also reported by some works in literature concerning sputtering of WS₂ target [9,12].

Fig. 2 shows GAXRD patterns obtained for WS_x, TiN, TiN-WS₄ and TiN-WS₁₉ samples. WS₂ and TiN patterns were confirmed using crystallographic data sheets ICDD PDF 08–0237 and ICDD PDF 38–1420, respectively. Despite sulfur deficiency, pure WS₂ sample showed two characteristic x-ray diffraction peaks referring to planes (101) and (112) of hexagonal structure, confirming the formation of WS₂ phase. Pure TiN sample presented a polycrystalline structure with preferential crystallographic orientation (111), consistent with other works in literature [9,22,23].

WS_x related peaks could not be identified in TiN-WS_x thin films

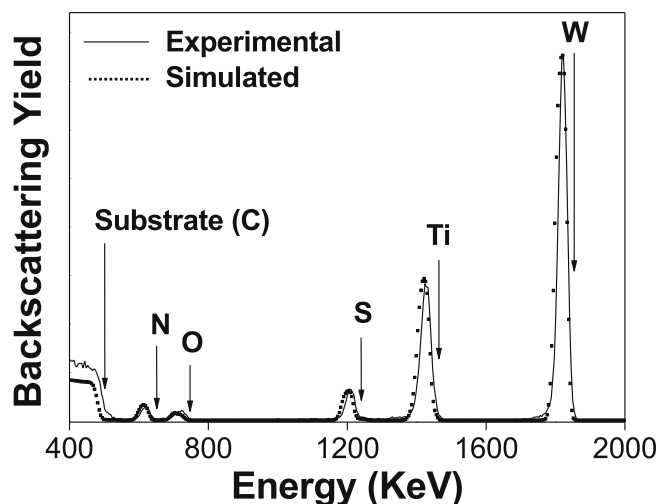


Fig. 1. RBS spectrum obtained for sample TiN with 19 at.% WS_x.

Table 1
Chemical elements concentration in WS_x, TiN and TiN-WS_x thin films.

Samples	Ti (at.%)	N (at.%)	W (at.%)	S (at.%)	[W/(W + Ti)]*100
WS _x	–	–	39.5	60.5	–
TiN	50.1	49.9	–	–	–
TiN-WS ₄	47.6	47.1	1.8	3.5	3.6
TiN-WS ₁₉	38.1	37.9	8.8	15.2	18.7

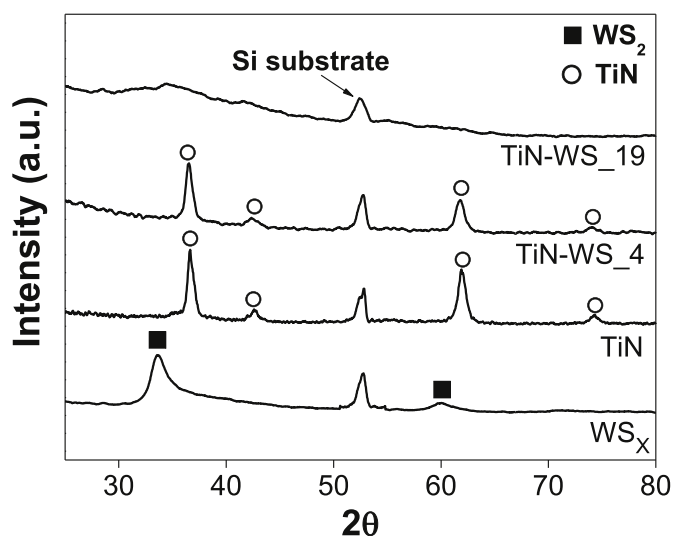


Fig. 2. GAXRD patterns for WS_x, TiN, TiN-WS₄ and TiN-WS₁₉ deposited on silicon substrate.

patterns. Nevertheless, it is possible to note that the addition of WS_x on sample TiN-WS₄ caused a reduction of TiN peaks intensity and a smooth broadening, indicating crystallite size decrease. Through Scherrer's equation, crystallite sizes were calculated for plane (111) and a reduction from 13.3 to 11.2 nm was observed for films of TiN and TiN-WS₄, respectively. The occurrence of such event is probably related to the increment of RF power applied to WS₂ target, seeing that crescent frequency of molecules impingement on the substrate generates a greater number of nucleating sites, which culminates in a reduced crystallite size.

Since only the peak related to silicon substrate can be identified in GAXRD pattern for sample TiN-WS₁₉, it is noticed that the increase of WS_x content transformed the TiN crystalline structure into amorphous. Thus, higher concentrations of WS_x inhibited the crystallization of TiN in the coatings.

Hardness values obtained through nanoindentation tests for silicon substrate and all samples are shown in Fig. 3. The registered average hardness value for Si substrate, TiN and WS_x samples were 5.1 GPa, 22.0 GPa and 3.8 GPa, respectively, coherent with values found in literature. It is noted that the addition of WS_x caused a gradual reduction in hardness results for samples TiN-WS₄ (19.7 GPa) and TiN-WS₁₉ (18.4 GPa). Not an occasional fact, since tungsten disulfide and titanium nitride are immiscible, TiN-WS_x results are closely followed by the rule of mixtures which culminates in intermediate hardness values for both samples. Further discussions about hardness will be correlated with tribological properties in the next chapter.

3.2. Tribological tests at room and high temperatures

TiN and TiN-WS_x thin films were deposited on AISI 304 stainless steel and tested with alumina (Al₂O₃) sphere as counter-body. Different friction coefficients (μ) were recorded, as shown in Fig. 4. Curve obtained for substrate is also described for comparative purposes, resulting in $\mu = 0.58$. For pure TiN sample, the acquired curve describes

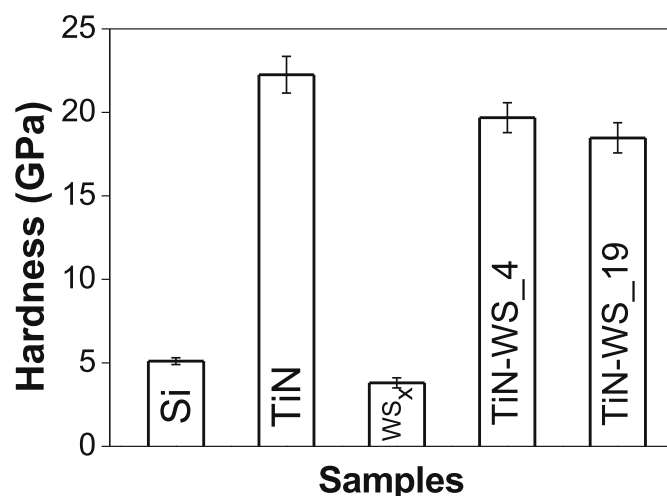


Fig. 3. Nanoindentation tests results of silicon substrate, TiN, WS_x, TiN-WS₄ and TiN-WS₁₉ samples.

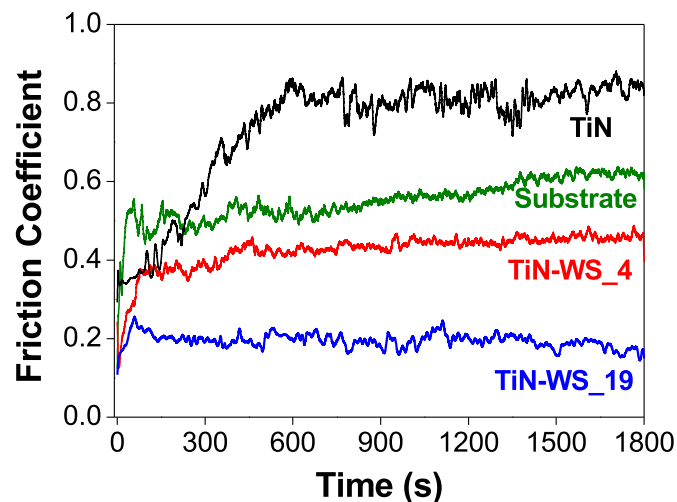


Fig. 4. Friction coefficients of substrate, TiN, TiN-WS₄ and TiN-WS₁₉ coatings at room temperature.

several fluctuations with average friction coefficient of $\mu = 0.79 \pm 0.09$, in agreement with literature [3]. On the other hand, TiN-WS₄ sample presented a friction coefficient curve with low fluctuations, with $\mu = 0.42 \pm 0.05$, representing a reduction of 50.6% when compared to pure TiN. This fact demonstrates the advantage of WS_x incorporation into TiN matrix, especially when it is considered that structure and hardness of the coating was comparable to that of TiN. In parallel, sample TiN-WS₁₉ presented a stable friction coefficient curve and low fluctuation levels, registering $\mu = 0.19 \pm 0.03$ (76% lower than pure TiN thin film). This substantial reduction in friction coefficient values indicates the establishment of effective lubricant action in the film associated with higher WS_x content.

Calculated wear rate provided by optic profiler within wear track for TiN thin film was $17.0 \times 10^{-17} \text{ m}^2/\text{N}$. For samples TiN-WS₄ and TiN-WS₁₉ that value diminished to 5.3×10^{-17} and $0.73 \times 10^{-17} \text{ m}^2/\text{N}$, respectively. Such decrease is attributed to friction coefficients reduction (Fig. 4) provided by solid lubricant associated with the conservation of high hardness values (Fig. 3).

Tribological tests with nanocomposite TiN-WS_x thin films were carried out at elevated temperatures reproducing previous tests conditions. Fig. 5 shows the friction coefficient curves for sample TiN-WS₄ under relative humidity of 60%. The curve referring to wear at 297 K is presented with comparative purposes. At 343 K, friction coefficient

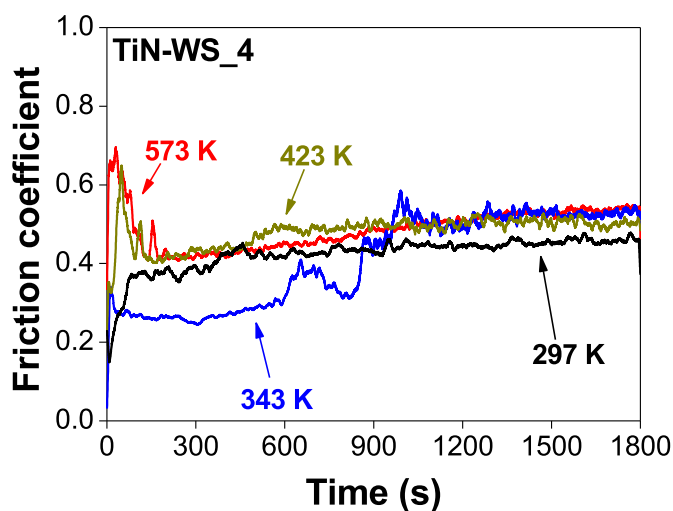


Fig. 5. Friction coefficients of TiN-WS₄ sample obtained at room temperature, 343 K, 423 K and 573 K.

remained ~ 0.25 until 586 s of test. The low friction effect verified at first probably occurs due to reduction of relative humidity in contact regions as a consequence of temperature increase, reaching nearly 10% [2,24]. Dry environments allow a more intense contact between sliding surfaces and diminishes the formation of tribo-oxidized thin films within the material interfaces [2,24,25], which favors solid lubricant WS_x effect. Subsequently, an accentuated raise in friction coefficient value was developed. That may be associated to probable disaggregation of particles by delamination and cracking of the coating [26], resulting in a final $\mu \sim 0.52$. Such value is near to friction coefficient of the substrate, indicating severe wear of thin films though maintaining some protective effect.

In tests executed at 423 and 573 K it is possible to notice a similarity between both resulting curves. At first, an intense variation in friction coefficient values is observed up to 200 s. That contrasts with the previous temperature, in which low values were initially registered due to humidity removal. As seen in the previous temperature, such accentuated variation is probably related to cracking of the coating. Therefore, severe conditions provided by increased temperature triggered thin film collapse as soon as sliding commenced. As a result, friction coefficients values of ~ 0.52 (near to AISI 304 substrate coefficient) were acquired once more.

Morphological analyses of wear zones obtained by SEM for TiN-WS₄ sample are shown in Fig. 6. At room temperature the surface presents characteristics of abrasive wear with the presence of soft micro-furrows (Fig. 6a). The surface tested at 343 K (Fig. 6b) showed a more intense abrasive wear with more pronounced furrows and adhesive debris. As shown by GAXRD and nanohardness tests results, addition of 4 at.% did not alter significantly TiN microstructure and hardness values. Thus, resulting wear tracks show brittle characteristics, with the formation of debris derived from cracks in the hard film structure which starts to participate in a three-body abrasion. Aforementioned features are directly related to fluctuations and the raise of friction coefficient presented in Fig. 5, where the substrate value was registered. The wear rate estimated by optical profiler was $5.3 \times 10^{-17} \text{ m}^2/\text{N}$, similar to room temperature value.

Samples TiN-WS₄ tested at 423 K also exhibited furrows and adhesion of residues (Fig. 6c). Moreover, superficial micro defects derived from debris production were observed. Such fact also relates to the raise of friction coefficient previously shown in Fig. 5. Interestingly, at 573 K (Fig. 6d) the wear zone presented surface flaws evidencing an increase in plastic deformation mechanism, what can be attributed to the temperature increase that commonly affects hardness and creep resistance [2,27,28]. Plastic deformation favors the establishment of furrows,

debris and delamination, partially exposing the substrate. Due to intensified abrasion the coating wear rates suffered a slight increment, registering values of $5.7 \times 10^{-17} \text{ m}^2/\text{N}$ and $6.2 \times 10^{-17} \text{ m}^2/\text{N}$ at 423 and 573 K, respectively.

The presence of constituent thin films materials in wear tracks was evaluated by EDS. Good tribological performance is suggested when iron or chromium related peaks from AISI 304 cannot be detected in wear tracks, meaning the substrate was not exposed and the film had no major modification in integrity after tribological tests. Fig. 7 shows EDS analyses obtained for sample TiN-WS₄ after tribological tests at different temperatures. Aluminum peak is attributed to Al₂O₃ counter-body residues. Peaks associated to titanium, tungsten and sulfur can be well identified in wear tracks obtained up to 343 K, indicating maintenance of thin film to some degree. Nevertheless, coatings tested at 423 and 573 K evidenced more intense iron related peaks, confirming major exposure of the substrate observed by SEM. Therefore, it is assumed that TiN-WS_x containing 4 at.% WS_x does not retain good tribological performance at temperatures above 343 K.

Friction coefficient curves for TiN-WS₁₉ samples are expressed in Fig. 8. The average value of friction coefficient at 343 K was $\mu = 0.23 \pm 0.06$, which is equivalent to the value obtained for this coating at room temperature ($\mu = 0.19 \pm 0.03$). In addition, it describes a well-stabilized friction coefficient curve with relatively low fluctuations, suggesting improved tribological properties at cited temperature due to maintenance of WS_x solid lubricant action. Such behavior differs from TiN-WS_x with 4 at.%, where good performance was maintained merely until 586 s of test. Therefore, amorphous character presented in section 3.1 for sample TiN-WS₁₉ reveals that, together with WS_x lubricious effect, crystallinity degree also plays a role in tribological properties at high temperatures.

On the other hand, at 423 K three stages with varied friction coefficient values can be clearly distinguished. Initially, average friction coefficient remained around 0.23 until 672 s, which may be associated to the effective action of solid lubricant favored by the complete removal of humidity from coating surface above 373 K [22,23]. However, throughout the test a drastic raise in friction coefficient occurred from approximately 700 s until 1400 s due to intense production of debris derived from delamination and ruptures. Thus, coefficient value was finally stabilized around ~ 0.59 , which is related to AISI 304 substrate. This behavior is very similar to that described for TiN-WS₄ sample at 343 K, nonetheless, since it was only manifested at a higher temperature, the additional WS_x content provided an improvement of wear resistance up to 423 K. At 573 K, an initially accentuated increase of friction and a subsequent variation in values that extends until approximately 300 s occurs. That is a similar behavior of TiN-WS₄ sample tested at this temperature. This stage is associated to coating deterioration and the stable values verified after 350 s is yet again associated to substrate friction coefficient. In other words, protection provided by the coating was not efficient in such high temperatures probably due to WS_x degradation [9,14].

Fig. 9 present morphological analyses of the wear track obtained for TiN-WS_x samples tested at high temperatures. At room temperature, topography showed low level of furrows, retaining predominant homogeneous aspects even after the test (Fig. 9a). Such behavior represents an improvement to TiN-WS₄ sample where a surface with more furrows was observed. At 343 K the surface aspect was similar to previous tested temperature, though a furrow of greater evidence in central region is evidenced (Fig. 9b). It is probably resulted from protrusions on the counter-body or abrasive residues from the sliding surfaces adhered on it. Wear rates obtained in this test was approximately $0.86 \times 10^{-17} \text{ m}^2/\text{N}$, slightly higher than that of room temperature ($0.73 \times 10^{-17} \text{ m}^2/\text{N}$). Nevertheless, it is considered an optimum value attributed to the good performance of WS_x under low humidity environments together with high hardness of the coating.

Topography of tribological tracks at 423 K (Fig. 9c) presented signs of residues adhesion and furrows of varied dimensions, characterizing

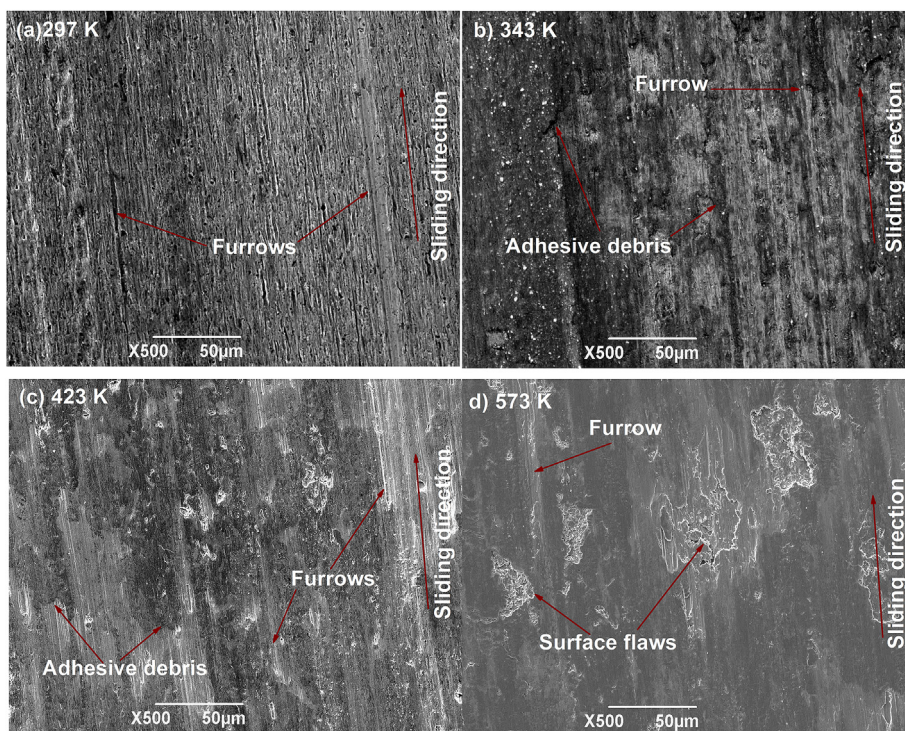


Fig. 6. SEM images of TiN-WS₄ wear zones at room temperature (a), 343 K (b), 423 K (c) and 573 K (d).

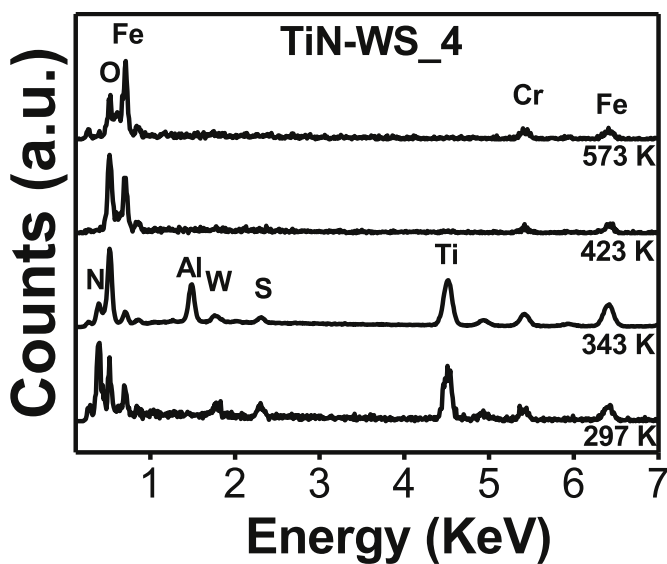


Fig. 7. EDS results of TiN-WS₄ wear zones.

an abrasive type of wear [26]. Those aspects can be attributed to fluctuations and raise in friction coefficients presented in Fig. 8 between 700 and 1400 s, evidencing the deterioration of the coating. Furthermore, an average wear rate of $4.90 \times 10^{-17} \text{ m}^2/\text{N}$ was acquired, indicating the reduction in wear resistance mainly when compared to tests executed at lower temperatures. Similarly, wear zone obtained from test at 573 K (Fig. 9d) also presented a surface with an intense abrasive wear, which elucidates the initial raise in friction coefficient values shown in Fig. 8. The estimated wear rate replicated the value of test at 423 K, what evidences the thin film deterioration in both experiments as seen by SEM micrographs.

EDS analyses inside wear track after tribological tests are shown in Fig. 10. At room temperature and at 343 K only constituent elements of the coatings were identified, with no Fe related peaks. That indicates

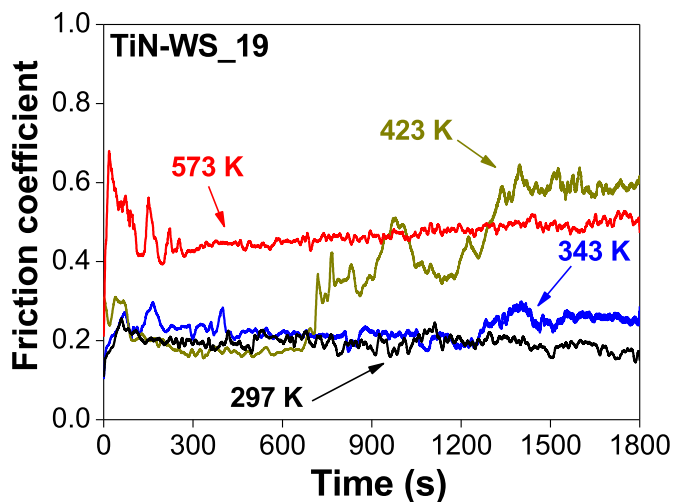


Fig. 8. Friction coefficients of TiN-WS₁₉ sample obtained at room temperature, 343 K, 423 K and 573 K.

the good tribological performance of TiN-WS₁₉ thin film up to 343 K, in agreement with homogeneous morphology seen by SEM images. Notwithstanding, sample tested at 423 K shows a reduction of intensity in peaks related to constituent elements and a simultaneous rise of iron peaks, suggesting the partial exposure of the substrate. Such fact was remarkably greater in sample tested at 573 K, in which a significant raise in substrate peaks intensity was detected. Thus, identified constituent elements are rather dispersed in debris along wear track and a greater exposure of the substrate occurs, as shown in SEM results.

4. Conclusions

TiN-WS_x thin films with varying WS_x content were successfully co-deposited by reactive magnetron sputtering. GAXRD analyses showed that the addition of 4 at.% WS_x led to the loss of crystallinity of TiN

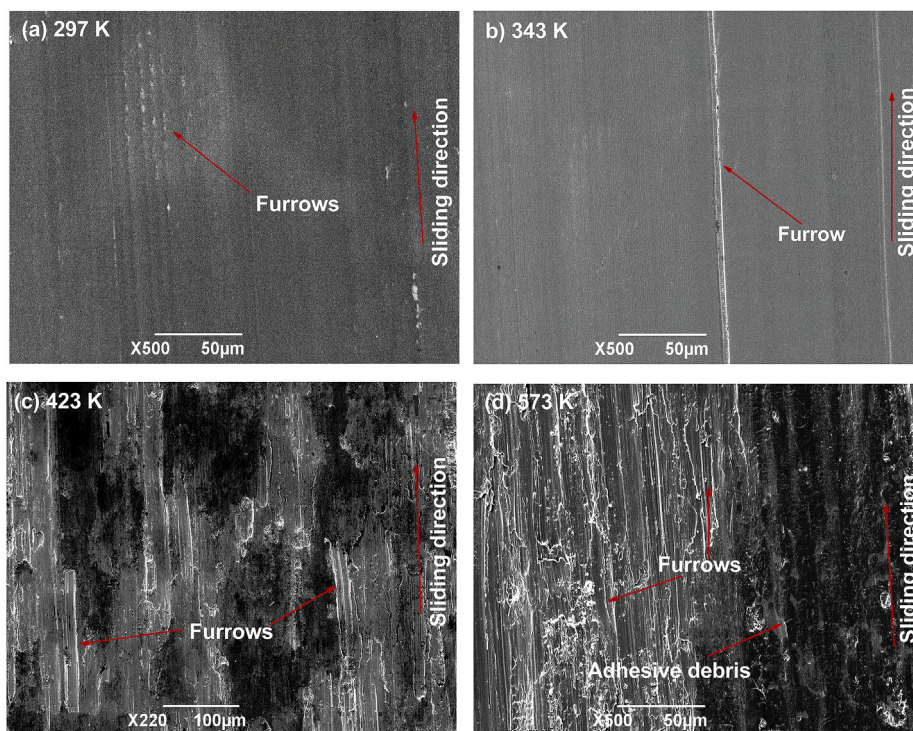


Fig. 9. SEM images of TiN-WS₁₉ wear zones at room temperature (a), 343 K (b), 423 K (c) and 573 K (d).

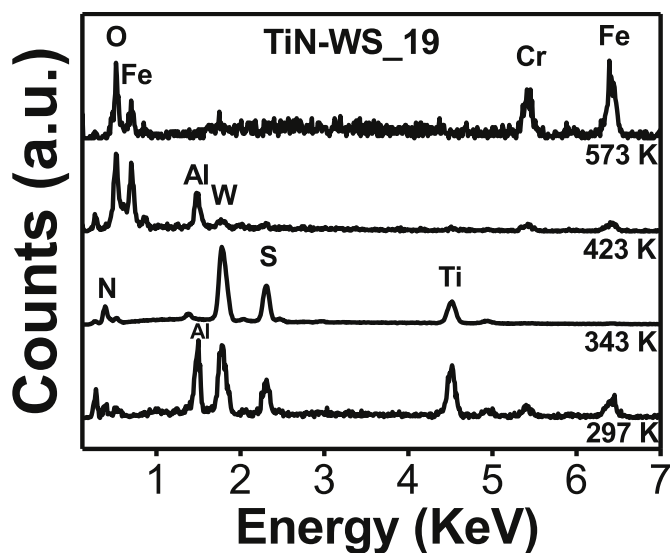


Fig. 10. EDS results of TiN-WS₁₉ wear zones.

phase and a complete amorphous characteristic was manifested upon incorporation of 19 at.% WS_x. Nanohardness results indicated that TiN-WS_x coatings present a tendency to follow the rule of mixtures.

Friction coefficient and wear rates measured in tribological tests revealed that TiN-WS_x presents a better tribological performance at room temperature than pure TiN. Wear tests at high temperatures evidenced that sample with 4 at.% WS_x did not preserve good tribological behavior registered for room temperature, on the other hand, coating with 19 at.% WS_x maintained good low friction coefficient up to 343 K. The more effective protection of the last nanocomposite is attributed mainly to the higher disulfide concentration associated to thin film amorphous characteristics, which showed a lower tendency to collapse.

Acknowledgements

The authors thank the UFRGS Ionic Implantation Laboratory for RBS analyses. This work was supported by CNPq, UEMA, CAPES and FAPITEC/SE.

References

- [1] D.-W. Tan, W.-M. Guo, H.-J. Wang, H.-T. Lin, C.-Y. Wang, Cutting performance and wear mechanism of TiB₂-B₄C ceramic cutting tools in high speed turning of Ti6Al4V alloy, *Ceram. Int.* 44 (13) (2018) 15495–15502, <https://doi.org/10.1016/j.ceramint.2018.05.209>.
- [2] E. Badisch, G. Fontalvo, M. Stoiber, C. Mitterer, Tribological behavior of PACVD TiN coatings in the temperature range up to 500 °C, *Surf. Coating Technol.* 163–164 (2003) 585–590, [https://doi.org/10.1016/S0257-8972\(02\)00626-6](https://doi.org/10.1016/S0257-8972(02)00626-6).
- [3] G. Strapasson, P.C. Badin, G.V. Soares, G. Machado, C.A. Figueroa, R. Hubler, A.L. Gasparin, I.J.R. Baumvol, C. Aguzzoli, E.K. Tentardini, Structure, composition, and mechanical characterization of dc sputtered TiN-MoS₂ nanocomposite thin films, *Surf. Coating Technol.* 205 (2011) 3810–3815, <https://doi.org/10.1016/j.surfcoat.2011.01.044>.
- [4] C. de L.R. Bottoni, M.C. Dias, L.C. Gontijo, Electrochemical behavior of titanium nitride thin films deposited on silicon by plasma discharge technique in cathodic cage, *Mater. Res.* 19 (2016) 1098–1101, <https://doi.org/10.1590/1980-5373-MR-2015-0241>.
- [5] S. Arun, S. Hariprasad, A. Saikiran, B. Ravisanakar, E.V. Parfenov, V.R. Mukaeava, N. Rameshbabu, The effect of graphite particle size on the corrosion and wear behaviour of the PEO-EPD coating fabricated on commercially pure zirconium, *Surf. Coating Technol.* 363 (2019) 301–313, <https://doi.org/10.1016/j.surfcoat.2019.02.033>.
- [6] X. Shi, T.W. Liskiewicz, B.D. Beake, J. Chen, C. Wang, Tribological performance of graphite-like carbon films with varied thickness, *Tribol. Int.* (2019), <https://doi.org/10.1016/j.triboint.2019.01.045>.
- [7] T. Hu, L. Hu, Tribological properties of lubricating films on the Al-Si alloy surface via laser surface texturing, *Tribol. Trans.* 54 (5) (2011) 800–805, <https://doi.org/10.1080/10402004.2011.604761>.
- [8] A.A. Voevodin, C. Muratore, S.M. Aouadi, Hard coatings with high temperature adaptive lubrication and contact thermal management: review, *Surf. Coating Technol.* 257 (2014) 247–265, <https://doi.org/10.1016/j.surfcoat.2014.04.046>.
- [9] T. Banerjee, A.K. Chattopadhyay, Structure, mechanical and tribological characterisations of pulsed DC magnetron sputtered TiN-WS_x composite coating, *Vacuum* 130 (2016) 93–104, <https://doi.org/10.1016/j.vacuum.2016.05.003>.
- [10] W.A. Brainard, The Thermal Stability and Friction of the Disulfides, Diselenides and Ditetellurides of Molybdenum and Tungsten in Vacuum (10⁻⁹ to 10⁻⁶ Torr), (1969) NASA TN D-5141.
- [11] T. Polcar, D.B. Mohan, C.S. Sandu, G. Radnoczi, A. Cavaleiro, Properties of

- nanocomposite film combining hard TiN matrix with embedded fullerene-like WS₂ nanoclusters, *Thin Solid Films* 519 (2011) 3191–3195, <https://doi.org/10.1016/j.tsf.2010.12.180>.
- [12] T. Banerjee, A.K. Chattopadhyay, Influence of substrate bias on structural and tribo-mechanical properties of pulsed magnetron sputtered TiN-WS₂ x hard-lubricious coating, *Tribol. Int.* 123 (2018) 81–91, <https://doi.org/10.1016/j.triboint.2018.03.005>.
- [13] Z. Li-na, W. Cheng-biao, W. Hai-dou, X. Bin-shi, Z. Da-ming, L. Jia-jun, L. Guo-lu, Tribological properties of WS₂ composite film prepared by a two-step method, *Vacuum* 85 (2010) 16–21, <https://doi.org/10.1016/j.vacuum.2010.03.003>.
- [14] S. Prasad, N. McDevitt, J. Zabinski, Tribology of tungsten disulfide–nanocrystalline zinc oxide adaptive lubricant films from ambient to 500°C, *Wear* 237 (2000) 186–196, [https://doi.org/10.1016/S0043-1648\(99\)00329-4](https://doi.org/10.1016/S0043-1648(99)00329-4).
- [15] M.A. Ezazi, M.M. Quazi, E. Zalnezhad, A.A.D. Sarhan, Enhancing the tribo-mechanical properties of aerospace AL7075-T6 by magnetron-sputtered Ti/TiN, Cr/CrN & TiCr/TiCrN thin film ceramic coatings, *Ceram. Int.* 40 (10) (2014) 15603–15615, <https://doi.org/10.1016/j.ceramint.2014.07.067>.
- [16] J.-F. Yang, B. Parakash, J. Hardell, Q.-F. Fang, Tribological properties of transition metal di-chalcogenide based lubricant coatings, *Front. Mater. Sci.* 6 (2012) 116–127, <https://doi.org/10.1007/s11706-012-0155-7>.
- [17] I. Hutchings, *Tribology: Friction and Wear of Engineering Materials, first ed.*, (1992) Boca Raton, Florida.
- [18] B. Deepthi, H.C. Barshilia, K.S. Rajam, M.S. Konchady, D.M. Pai, J. Sankar, Structural, mechanical and tribological investigations of sputter deposited CrN-WS₂ nanocomposite solid lubricant coatings, *Tribol. Int.* 44 (2011) 1844–1851, <https://doi.org/10.1016/j.triboint.2011.07.007>.
- [19] S. Sharma, S. Sangal, K. Mondal, On the optical microscopic method for the determination of ball-on-flat surface linearly reciprocating sliding wear volume, *Wear* 300 (2013) 82–89, <https://doi.org/10.1016/j.wear.2013.01.107>.
- [20] M.A. Signore, A. Rizzo, L. Mirengi, M.A. Tagliente, A. Cappello, Characterization of zirconium oxynitride films obtained by radio frequency magnetron reactive sputtering, *Thin Solid Films* 515 (2007) 6798–6804, <https://doi.org/10.1016/j.tsf.2007.02.033>.
- [21] P.C. Silva Neto, F.G.R. Freitas, D.A.R. Fernandez, R.G. Carvalho, L.C. Felix, A.R. Terto, R. Hubler, F.M.T. Mendes, A.H. Silva Junior, E.K. Tentardini, Investigation of microstructure and properties of magnetron sputtered Zr-Si-N thin films with different Si content, *Surf. Coating. Technol.* 353 (2018) 355–363, <https://doi.org/10.1016/j.surfcoat.2018.07.106>.
- [22] I. Iordanova, P.J. Kelly, M. Burova, A. Andreeva, B. Stefanova, Influence of thickness on the crystallography and surface topography of TiN nano-films deposited by reactive DC and pulsed magnetron sputtering, *Thin Solid Films* 520 (2012) 5333–5339, <https://doi.org/10.1016/j.tsf.2012.03.097>.
- [23] D. Martínez-Martínez, C. López-Cartes, A. Fernández, J.C. Sánchez-López, Exploring the benefits of depositing hard TiN thin films by non-reactive magnetron sputtering, *Appl. Surf. Sci.* 275 (2013) 121–126, <https://doi.org/10.1016/j.apsusc.2013.01.098>.
- [24] P.J. Blau, Elevated-temperature tribology of metallic materials, *Tribol. Int.* 43 (2010) 1203–1208, <https://doi.org/10.1016/j.triboint.2010.01.003>.
- [25] T. Polcar, A. Cavaleiro, Review on self-lubricant transition metal dichalcogenide nanocomposite coatings alloyed with carbon, *Surf. Coating. Technol.* 206 (2011) 686–695, <https://doi.org/10.1016/j.surfcoat.2011.03.004>.
- [26] P. Chen, X. Xiang, T. Shao, Y. La, J. Li, Effect of triangular texture on the tribological performance of die steel with TiN coatings under lubricated sliding condition, *Appl. Surf. Sci.* 389 (2016) 361–368, <https://doi.org/10.1016/j.apsusc.2016.07.119>.
- [27] A.P. Semenov, Tribology at high temperatures, *Tribol. Int.* 28 (1995) 45–50, [https://doi.org/10.1016/0301-679X\(95\)99493-5](https://doi.org/10.1016/0301-679X(95)99493-5).
- [28] R. Niu, J. Li, Y. Wang, J. Chen, Q. Xue, Structure and high temperature tribological behavior of TiAlN/nitride duplex treated coatings on Ti6Al4V, *Surf. Coating. Technol.* 309 (2017) 232–241, <https://doi.org/10.1016/j.surfcoat.2016.05.016>.